Paper-Strip Sculptures

Ergun Akleman[1], Jianer Chen[2], Jonathan L. Gross[3]
[1]Visualization Department, Texas A&M University
[2]Computer Science Department, Texas A&M University
[3]Computer Science Department, Columbia University

***Abstract*—This paper introduces paper-strip sculptures, a physical mesh data-structure used to represent 2-manifold mesh surfaces for understanding topological and geometrical aspects of shape modeling with visual and tactual examples. With paper strips it is possible to construct simple paper sculptures that can convincingly illustrate a variety of ideas in shape modeling — such as 2-manifold mesh surfaces, discrete Gaussian curvature, and the Gauss-Bonnet theorem — with hands-on experiments. Such sculptures can also represent links, knots and weaving. Paper-strip sculptures are also useful to represent and understand non-orientable surfaces such as the projective plane and the Klein bottle.**

***Keywords*-Shape Modeling, Mesh Data Structures, Topology and Geometry, Discrete Gaussian Curvature, Gauss-Bonnet Theorem.**

1. Introduction and Motivation

In this paper, we present a simple way to construct paper sculptures that can illustrate a wide variety of concepts related to geometric modeling. These paper sculptures are conceptualized as data structures that can easily be constructed by combining strips of paper. We call these structures *paper-strip structures*. These paper-strip sculptures are 3D representations of the band structures introduced by Gross and Tucker to represent 2-manifold mesh surfaces [1]. In addition to the power of band structures for representing the topological nature of 2-manifold mesh surfaces, paper-strip sculptures provide visual and tactual intuition for important geometric concepts, such as discrete Gaussian curvature (face-defect) and the Gauss-Bonnet theorem.

Paper strips are a powerful tool for teaching difficult geometric modeling concepts with tangible examples. They are also useful for research, because of their simplicity and immediacy. For instance, some of our ideas for studying links started from paper-strip structures. We have revised some existing surgery theorems of topological graph theory based on our observations from paper strips. Our theoretical results in this regard appear in [2] and [3].

2. Definitions

Paper-strip sculptures are assembled from a set of strips of paper by using various types of connectors, such as staples, tape, glue, sew-on snaps, or brass fasteners. For uniform appearance and cleanly cut paper strips (as in Figure 1(a)), we use laser cutting.

For experimenting with paper-strip sculptures, we prefer metallic connectors, since they allow changing the angle between two strips by freely rotating around the connection points. Moreover, using metallic connectors permits reuse of the paper strips. On the other hand, to construct a final structure, it is helpful to use staples, tape, or glue to fix the cyclic order of the paper strips incident at each of the connectors. Figure 1(b) shows a pair of sew-on snaps. Figure 1(c) shows three round-head brass fasteners.

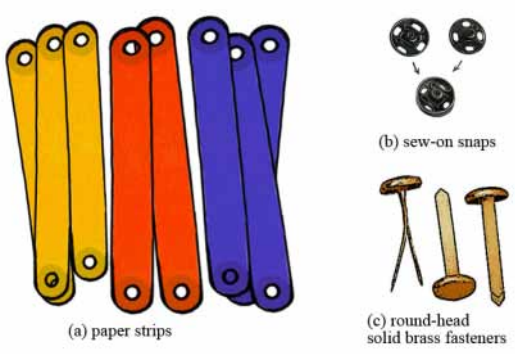

Fig. 1. *Basic elements of paper-strip sculptures are the paper strips and the connectors, such as sew-on snaps and brass fasteners.*

To construct the visual sculptures in the figures of this paper, we used paper strips that were cut by a laser cutter. To get the images for our figures, we first photographed the paper sculptures. We then improved the visual quality of photographs by re-painting over the photographs. Unfortunately, even with our improvements, the photographs fail to provide the complete visual and tactual power of the paper sculptures. Therefore, we strongly suggest building them to experience first-hand the power of these sculptures.

2.1 Finger Traversing a Boundary Walk

Let $\mathcal{P}$ be a paper-strip sculpture that is constructed (in 3D-space) by connecting a set of paper strips, some of which may be twisted. We envision an extension from the surface of sculpture $\mathcal{P}$ to a closed 2-manifold $\mathcal{S}$, such that $\mathcal{P} - \mathcal{S}$ consists of a set of non-intersecting open disks. Such an extension always exists (but not necessarily in Euclidean 3D-space), and the extension induces a cellular decomposition of the 2-manifold $\mathcal{S}$. To traverse a boundary component in a paper-strip sculpture, one can put a finger on the edge of one of the paper strips and trace forward (i.e., without reversal) until returning to the starting position, as shown in Figure 2.

(a) Toroid. (b) Finger's Trajectory (c) Open cell.

Fig. 2. *A face-boundary walk can be traversed with a finger. (b) shows the finger trajectory. (c) shows that it is possible to insert a stretchable rubber disk into space, whose boundary is matched to that boundary cycle of the paper sculpture.*

The finger trajectory can be a complicated space curve, even for simple examples such as the toroidal shape shown in Figure 2. This toroidal shape is represented by a paper sculpture built from two paper strips and one connector, as shown in Figure 2(a). The image in (b) shows the finger trajectory along the only boundary component of the sculpture. Thus, the (invisible) extension to a closed surface requires only one 2-cell, which caps off that one boundary component. By physically finger-traversing the boundary of a paper-strip sculpture, one may be able to see that the boundary cycle is unknotted in space, which is a necessary condition for it to be possible to insert a stretchable rubber disk into space whose boundary is matched to that boundary cycle of the paper sculpture. Figure 2(c) shows an extension of Figure 2(a) to a torus.

3. Topological Properties

Two paper-strips in a sculpture are said to be *adjacent* if they meet at a connector. Some sequences of adjacent paper strips form closed walks within the sculpture. A paper-strip sculpture and its associated closed surface are non-orientable if any of these closed walks forms a Möbius band. Otherwise the sculpture and its associated surface are orientable. (See the Orientability Algorithm for band decompositions in [1].)

Alternatively, we can paint one side of each paper-strip. If there is no connector at which a painted side of some strip meets an unpainted side of some other strip (or of the same strip) then the surface is certainly orientable. On the other hand, in non-orientable surfaces such as a Klein bottle, we would have to paint both sides of each strip to avoid having a painted side meet an unpainted side.

In general, the Euler characteristic of the surface represented by a paper-strip sculpture $\mathcal{P}$ has the Euler characteristic $\chi(\mathcal{P}) = V - E$ where V is the number of connectors and E is the number of paper strips. The Euler characteristic of the corresponding closed surface $\mathcal{S}$ is $\chi(\mathcal{S}) = V - E + F$, where F is the number of boundary components of $\mathcal{P}$.

Finger-traversing the boundary of a face remains easy even when the surface is non-orientable. Figure 3 illustrates the space curves resulting from finger-traversals of the face boundary of a projective plane (a0) and of a Klein bottle (a1). The projective plane (non-orientable genus-1) in (a0) has one paper strip, one connection point, and only one 2-cell. The Klein bottle (non-orientable genus-2) in (a1) consists of two paper strips, one connection point, and only one cell. The images in (b0) and (b1) show the trajectory of a finger tip. These single faces again are conceptualized by disks that are bounded by the finger-trajectories, but whose immersion in 3D-space without intersections is impossible, even though the finger trajectories are unknotted closed curves in 3D-space. In other words, unknottedness of a boundary component of the surface represented by the paper sculpture is not sufficient to avoid intersections. Closed non-orientable 2-manifolds in 3D-space necessarily have self-intersections. These paper-strip sculptures provide an alternative representation in which self-intersection is avoided.

(a0) (b0) (a1) (b1)

Fig. 3. *Finger trajectories for boundary walk of non-orientable surfaces. (a0) and (b0) are projective plane and finger's trajectory for projective plane. (a1) and (b1) are Klein bottle and the corresponding finger's trajectory.*

3.1 Relation with Graph Rotation Systems

Graph Rotation Systems have been a powerful model in the study of topological graph theory [1], [4], [5], [6]. A *rotation at a vertex* of a graph is a cyclic ordering of the set of the edge-ends that are incident at that vertex. A *rotation system* for a graph consists of a rotation at every vertex. It is well-known (see Theorem 3.2.2 of [1]) that a rotation system specifies a graph embedding. The abstract mathematical properties of Graph Rotation Systems can be realized and analyzed visually and tactually using paper-strip sculptures, which are similar to the band-decomposition structure studied in topological graph theory [1]. They are also helpful for discovering properties that are either not known or not well-understood previously.

A most useful property of paper-strip sculptures to explain mesh data structures is their amenability to finger-tracing of the face boundaries. This finger-tracing process explains how a graph rotation system specifies an embedding in a closed surface [1]. By assuming that each paper-strip is a representation of a regular neighborhood of an edge of the graph, and that each connection point of the paper strips represents a vertex, the 2-cells (i.e. disks) become the faces of the extension of $\mathcal{P}$ to a closed surface. The cyclic order of the edge-ends incident at a vertex is always well-defined and visually clear in a paper-strip model. The set of paper strips that are connected together form a planar region around the connection point. Therefore, we can always see the cyclic order of the edge-ends in that planar region.

3.2 Relation with Polygonal Data Structures

Paper-strip sculptures are especially useful for 3D visualization and tactualization of topological properties of polygonal data structures. The long sides of a strip represent half-edges, in the sense of [7]. Cyclically ordered sets of half-edges represent faces, and a set of ordered edge-ends represents a vertex. The two holes at the ends of a strip can be considered edge-ends [8]. Paper strips also correspond to quadedges, in the sense of [9]. Akleman et al. showed that starting from a set of vertex-manifolds, any orientable or non-orientable manifold mesh can be constructed by inserting and twisting edges [10]. To be able to insert an edge into a paper-strip structure, we first need to define the concept of a corner.

Definition A *corner* of a paper-strip sculpture is specified as a triple containing one side of a paper strip, one side of another paper strip, and a connector that joins the two paper strips so that the designated sides of the two paper strips are locally on the same side of the surface, and consecutive in the cyclic order at that connector. If there is no paper-strip, the corner is just a connector. Rotation order of the strips at the connector is consistent with the rotation order around the connector (i.e., vertex). The number of corners at a connector equals the number of paper-strip ends incident at that connector.

3.3 Links and Weaving

Akleman et al. noticed that the boundary walks induced by a graph rotation system define a link in 3D-space, and they used this property to construct plain-weaving cycles on arbitrary polygonal mesh surfaces [3], [2]. This insight can be realized visually using paper-strip sculptures, as shown in Figure 4. Figure 4(a) gives an octahedron constructed by paper strips, embedded in a sphere. As shown in Figure 4(b), the eight face-boundary walks of the octahedron are unlinked in 3D-space. However, if the edges are twisted as shown in Figure 4(c), then the cycles represented by the boundary walks become linked, as in Figure 4(d).

Whereas the standard band decompositions [1] used by topological graph theorists model the twisting on a band modulo 2 (i.e., as twisted or untwisted), our extended band decompositions model the twisting over the integers (For more information on integer twisting see [2]). Not only the number of twists matters, but also the orientation of the twists matters. As a simple example, consider twists on a band decomposition corresponding to the graph C_3, the 3-cycle. If the three bands have twists 1, 2, and 2, then the knot obtained is 5_1. If the twists are -1, 2, 2, then the knot is 3_1, the trefoil. If the twists are 1, -2, 2, the result is an unknot.

4. Geometric Properties

With paper-strip sculptures, it is possible to assign geometric information to the topological entities such as corners. Such information is useful to teaching geometrical concepts, e.g. discrete Gaussian curvature and the Gauss-Bonnet theorem. In paper strip sculptures, the most useful geometric entity is the corner angle, which we have defined as follows.

(a) (b) (c) (d)

Fig. 4. *The boundary walks of paper-strip sculptures are links in 3D space.*

Definition A *corner angle* θ is the angle between two imaginary lines passing through the centers (lengthwise) of the ends of two paper strips that are consecutive at a corner. The sum of all the corner angles around a vertex is always 2π, since the strips are locally flat around the vertex. The size of this locally flat area depends on the stiffness of the paper and it is usually much larger than the width of the paper strips. Therefore, the angle between two half-edges of a corner is the same as the corner angle, and it is always possible to use the angle between two half-edges as the corner angle since the paper strips do not bend much around the vertex.

4.1 Discrete Gaussian Curvature and Face-Defect

Paper strips are developable surfaces, with zero Gaussian curvature. Moreover, since around a vertex a paper-strip surface is also locally flat, the Gaussian curvature of our sculptures is also zero around the vertices. Accordingly, all the Gaussian curvature exists in the empty spaces that correspond to faces. We define ϕ, the discrete Gaussian curvature of a face, or *face-defect*, for an n-sided face, as

$$\phi = \sum_{i=0}^{n} \theta_i - (n-2)\pi$$

where θ_i is the angle at corner i. Of course, $(n-2)\pi$ is the sum of the angles if the polygon is planar. In other words, the face-defect is a measure of how much a polygon deviates from a flat surface. If the sum of the internal angles of the triangle is exactly π, then the result becomes a flat triangle. However, as soon as we increase the sum of the internal angles, the triangle becomes curved, and it becomes easy to imagine that the triangle is drawn on a surface of a sphere.

Note that we can categorize the shapes of the faces, based on face-defect.

- If the face-defect is zero, then either the face is flat or the Gaussian curvatures inside of the face cancel each other. This means that the polygon is either drawn on a flat surface or it is a part of a toroidal or cylindrical shape. It is also possible to call such a polygon a *Euclidean polygon*.
- If the face-defect is positive, then the face has a convex

or a concave shape. It is possible to call such polygons *elliptic*. An interesting case is when every angle is π, implying that $\phi = 2\pi$, in which case the polygon forms a circular band.

• If the face-defect is negative, then the face has a saddle shape. We call such polygons *hyperbolic*, and they can be drawn on a surface of negative curvature.

These cases are illustrated in Figure IV-A. Note that these shapes were created from each other by simply changing the sums of the internal angles of the polygons formed by paper strips. Changing the internal angles is easy using simple connectors, since the paper strips can rotate freely around the snaps.

Positive Negative Positive Negative

(a) Triangles (b) Quadrilaterals

Fig. 5. *Triangles and Quadrilaterals. (a) shows triangles with positive and negative Gaussian curvature. (b) shows squares with positive and negative Gaussian curvature.*

4.2 Illustrating Monogons and Digons with Face-Defect

Another interesting concept to teach is polygons with only one or two vertices, which are called monogons and digons. Such polygons can frequently occur during the modeling stage. However, they are non-realizable if we render the edges as straight lines. By representing edges with flexible paper strips, these type of polygons becomes much more understandable, as shown in Figure 6. Note that for flat polygons, the sum of the internal corner angles is $(n-2)\pi$. For digons, this sum is zero; thus, each corner angle has to be zero for flat digons. This case is shown in Figure 6(a). On the other hand, for a monogon, the sum of the internal angle must be $-\pi$. In other words, a flat monogon does not exist, and therefore we do not have an example in Figure 6(b).

Positive Positive Zero Positive Positive

(a)Digons (b) Monogons

Fig. 6. *Monogons and Digons. (a) shows monogons, which always have positive curvature. (b) shows digons, which can have zero curvature but the result appears as a straight line.*

4.3 Regular Meshes and Maps

Regular meshes are special types of meshes in which every vertex has the same valence and every face has the same number of sides. A regular mesh is represented by a triple (n, m, g), where n is the face size, m is the vertex valence, and g is the genus of the surface [11]. A very interesting subset of regular meshes are Coxeter's regular maps, which are defined by an additional set of symmetry conditions [12], [13]. The regular maps of genus smaller than 100 have recently been by cataloged by Conder [14], [15]. Van Wijk recently developed a method to visualize a large subset of the regular maps [16]. Paper strips provide a very useful and intuitive tool to construct regular meshes and regular maps. If one simply chooses the required vertex valences, the number of sides of the faces, and the face-defects, then paper strips connected by fasteners can be used to form a symmetrical shape. We have tried constructing some shapes, and the process is simple and educational. We did not include any figures here, since the photographs of paper strips with large holes do not indicate the real power of these sculptures. We strongly urge the readers to build their own regular meshes or maps to experience these interesting structures.

4.4 Illustrating Gauss-Bonnet Theorem with Examples

One of the fortuitous properties of paper-strip sculptures is that they can be used to illustrate the Gauss-Bonnet Theorem [17]. The Gauss-Bonnet Theorem implies that for a manifold mesh $\mathcal{M}$, the sum of the face-defects must be equal to 2π times $\chi(\mathcal{M})$, the Euler characteristic of the corresponding surface. For instance, for a genus-0 manifold mesh, this sum must be equal to 4π. Using a set of faces whose face-defects sum to 4π, we can create ball-like shapes. On the other hand, for genus-1 surfaces, the Euler characteristic is zero; therefore, the face-defects must sum to 0. In this section, we examine three genus-0 examples, which are depicted in Figure 7, and also a toroid, with genus 1.

(a) Tetrahedron (b) Octahedron (c) Cube $(4, 3, 0)$

Fig. 7. *Paper-Strip Representations of Platonic Solids*

Platonic Solids: Platonic solids correspond to regular meshes where $g = 0$, $n > 2$ and $m > 2$. Using Euler characteristic, we can compute the number of the faces of a platonic solid as $F = 4m/(2m + 2n - nm)$. To create the ball-like sculptures shown in Figure 7(a), (b) and (c), we can introduce face-defect $4\pi/F$ for each face, with the sum 4π of all the face-defects distributed evenly over the F number of faces. Each face of the platonic solid is n-sided, and the sum of the internal angles for a flat triangle is $(n-2)\pi$. It follows that the sum of all the angles for such positively curved triangle must be $(n-2)\pi + 4\pi/F = 2n\pi/m$. If all the internal

angles are equal, then each of the three internal angles has to be $\theta_i = 2\pi/m$. Thus, by choosing each internal angle to be $2\pi/m$, we obtain the sculptures shown in Figure 7(a), (b) and (c).

Regular Toroids: To create the toroidal shapes in Figure 8, we can introduce face-defect zero for each face, since for genus-1 surfaces the Euler characteristic is zero. All the faces of all the illustrated toroidal shapes are quadrilaterals, and the sum of the internal angles for a flat quadrilateral is 2π. Of course, the sum of all the angles for a zero-curvature quadrilateral must be 2π. If all the internal angles are equal, then each internal angle of a quadrilateral is $\pi/2$. It follows that by choosing each internal angle to be $\pi/2$, we can obtain the sculptures shown in Figure 8(a), (b) and (c). Note that in these three cases, all the quadrilaterals are exactly the same. This is particularly interesting, since we have both positive and negative curvatures that cancel each other, for a total curvature of zero, and we end up with a structure with 90^0 corner angles, exactly like a square, but the results are toroidal sculptures. On the other hand, it is also possible to build toroidal shapes using positively and negatively curved faces as shown in Figure 8(d). In this particular example, we have two types of quadrilaterals: one set of quadrilaterals has positive curvature, and the other set has negative curvature, so the total Gaussian curvature is 0. Such exercises can be particularly helpful to understand the distribution of the Gaussian curvature on the surface.

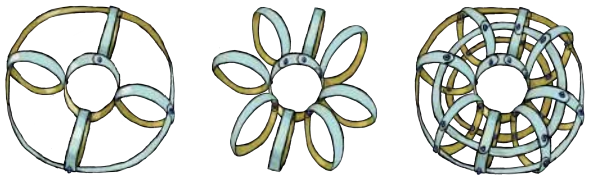

(a) Four faces (b) Eight faces (d) 32 faces

Fig. 8. *Four different Paper-Strip Representations of* $(4, 4, 1)$ *Toroidal Shapes* .

4.5 Duality

We observe that paper-strip sculptures are a form of geometric dual to polyhedral meshes, such as the widely used triangular meshes. In polyhedral meshes, every face is planar and every edge is straight. Therefore, the discrete Gaussian curvature of every face and edge is zero, and non-zero Gaussian curvature exists only at vertices. When we take the dual of a mesh, the vertices become faces and the faces becomes vertices. In the dual, therefore, non-zero discrete Gaussian curvature of the dual mesh should exist only at faces. Since paper-strip sculptures exactly provides this property, we may regard paper-strip sculptures as an authentic dual of polyhedral meshes. For instance, the dual of any triangular mesh can be represented by a paper-strip sculpture in which every vertex is 3-valent.

There is a further implication of this perspective, coming from a duality that exists between physical and virtual representations. We all know that triangular meshes are popular in computer graphics, since they are easy to construct virtually. However, it is hard to construct triangular meshes physically, because of the conical-mesh property [18]. On the other hand, paper strips are very easy to construct physically, since physical constraints are automatically satisfied. Since paper-strip sculptures can represent duals of triangular meshes, It follows that large sculptural or architectural shapes can be constructed using paper-strip sculptures, by replacing paper with thin metal sheets from triangular meshes that are modeled virtually.

REFERENCES

[1] J. L. Gross and T. W. Tucker, *Topological Graph Theory*. Wiley Interscience, New York, 1987.

[2] E. Akleman, J. Chen, J. Gross, and Q. Xing, "Extended graph rotation systems as a model for cyclic weaving on orientable surfaces," Technical Report - Computer Science Department, Texas A&M University - TR09-203, 2009.

[3] E. Akleman, J. Chen, Q. Xing, and J. Gross, "Cyclic plain-weaving with extended graph rotation systems," *ACM Transactions on Graphics; Proceedings of SIGGRAPH'2009*, pp. 78.1–78.8, 2009.

[4] A. T. White, *Graphs of Groups on Surfaces, Volume 188: Interactions and Models*. North-Holland Mathematics Studies, 2001.

[5] C. P. Bonnington and C. H. C. Little, *The Foundations of Topological Graph Theory*. Springer, New York, 1995.

[6] J. Chen, J. L. Gross, and R. G. Rieper, "Overlap matrices and total imbedding distributions," *Discrete Mathematics*, no. 128, pp. 73–94, 1994.

[7] M. Mantyla, *An Introduction to Solid Modeling*. Computer Science Press, Rockville, Ma., 1988.

[8] E. Akleman and J. Chen, "Guaranteeing the 2-manifold property for meshes with doubly linked face list," *International Journal of Shape Modeling*, vol. 5, no. 2, pp. 149–177, 1999.

[9] L. Guibas and J. Stolfi, "Primitives for the manipulation of general subdivisions and computation of voronoi diagrams," *ACM Transaction on Graphics*, no. 4, pp. 74–123, 1985.

[10] E. Akleman, J. Chen, and V. Srinivasan, "A minimal and complete set of operators for the development of robust manifold mesh modelers," *Graphical Models Journal, Special issue on International Conference on Shape Modeling and Applications 2002*, vol. 65, no. 2, pp. 286–304, 2003.

[11] E. Akleman and J. Chen, "Regular mesh construction algorithms using regular handles," in *Proceedings of IEEE Int. Conference on Shape Modeling and Applications, (SMI 06)*, 2006, pp. 171–181.

[12] H. Coxeter, *Introduction to Geometry*. Wiley, 1989.

[13] H. Coxeter and W. Moser, *Generators and Relations for Discrete Groups*. Springer-Verlag, Berlin, 1984.

[14] M. Conder and P. Dobcsny, "Determination of all regular maps of small genus," *Journal of Combinatorial Theory*, pp. 224–242, 2001.

[15] M. Conder, "Orientable regular maps of genus 2 to 101," http://www.math.auckland.ac.nz/~conder, 2006.

[16] J. V. Wijk, "Symmetric tiling of closed surfaces: Visualization of regular maps," *ACM Transactions on Graphics; Proceedings of SIGGRAPH'2009*, pp. 49.1–49.12, 2009.

[17] E. Akleman and J. Chen, "Practical polygonal mesh modeling with discrete gauss-bonnet theorem," in *Proceedings of Geometry Modeling and Processing (GMP'06)*, 2006, pp. 287–298.

[18] Y. Liu, H. Pottmann, J. Wallner, Y. Yang, and W. Wang, "Geometric modeling with conical meshes and developable surfaces," *ACM Transactions on Graphics; Proceedings of SIGGRAPH'2006*, pp. 681–689, 2006.